Chloroplast remodeling during state transitions in *Chlamydomonas reinhardtii* as revealed by noninvasive techniques in vivo

Gergely Nagy[a,b,c], Renáta Ünnep[b], Ottó Zsiros[d], Ryutaro Tokutsu[e,f], Kenji Takizawa[e], Lionel Porcar[c], Lucas Moyet[g,h,i,j], Dimitris Petroutsos[g,h,i,j], Győző Garab[d,1], Giovanni Finazzi[g,h,i,j,1], and Jun Minagawa[e,f,1]

[a]Laboratory for Neutron Scattering, Paul Scherrer Institute, 5232 Villigen PSI, Switzerland; [b]Wigner Research Centre for Physics, Institute for Solid State Physics and Optics, Hungarian Academy of Sciences, H-1525, Budapest, Hungary; [c]Institut Laue-Langevin, BP 156, F-38042 Grenoble Cedex 9, France; [d]Institute of Plant Biology, Biological Research Center, Hungarian Academy of Sciences, H-6701, Szeged, Hungary; [e]Division of Environmental Photobiology, National Institute for Basic Biology, Nishigonaka 38, Myodaiji, Okazaki 444-8585, Japan; [f]CREST, Japan Science and Technology Agency, 4-1-8 Honcho, Kawaguchi 332-0012, Japan; [9]Laboratoire de Physiologie Cellulaire et Végétale, Unité Mixte de Recherche 5168, Centre National de la Recherche Scientifique, F-38054 Grenoble Cedex 9, France; [h]Université Grenoble Alpes, F-38054 Grenoble Cedex 9, France; [i]Institut National Recherche Agronomique, F-38054 Grenoble Cedex 9, France; and [j]Institut de Recherche en Sciences et Technologie du Vivant, Commissariat à l'Energie Atomique et aux Energies Alternatives (CEA) Grenoble, F-38054 Grenoble Cedex 9, France

Edited by Elisabeth Gantt, University of Maryland, College Park, MD, and approved February 25, 2014 (received for review December 4, 2013)

Plants respond to changes in light quality by regulating the absorption capacity of their photosystems. These short-term adaptations use redox-controlled, reversible phosphorylation of the light-harvesting complexes (LHCIIs) to regulate the relative absorption cross-section of the two photosystems (PSs), commonly referred to as state transitions. It is acknowledged that state transitions induce substantial reorganizations of the PSs. However, their consequences on the chloroplast structure are more controversial. Here, we investigate how state transitions affect the chloroplast structure and function using complementary approaches for the living cells of *Chlamydomonas reinhardtii*. Using small-angle neutron scattering, we found a strong periodicity of the thylakoids in state 1, with characteristic repeat distances of ∼200 Å, which was almost completely lost in state 2. As revealed by circular dichroism, changes in the thylakoid periodicity were paralleled by modifications in the long-range order arrangement of the photosynthetic complexes, which was reduced by ∼20% in state 2 compared with state 1, but was not abolished. Furthermore, absorption spectroscopy reveals that the enhancement of PSI antenna size during state 1 to state 2 transition (∼20%) is not commensurate to the decrease in PSII antenna size (∼70%), leading to the possibility that a large part of the phosphorylated LHCIIs do not bind to PSI, but instead form energetically quenched complexes, which were shown to be either associated with PSII supercomplexes or in a free form. Altogether these noninvasive in vivo approaches allow us to present a more likely scenario for state transitions that explains their molecular mechanism and physiological consequences.

green algae | photosynthesis | thylakoid membrane

The efficient operation of the photosynthetic machinery of oxygenic photosynthetic organisms requires a balanced energy supply to the two photosystems (PSs) under changing environments. To avoid unbalanced excitations of the two PSs, a rapid acclimation mechanism, state transitions (STs), takes place, which allows redistributing the excitation energy between the two PSs. ST is seen in green algae and vascular plants and is modulated by the redox-controlled, reversible phosphorylation of LHCII, the light-harvesting chlorophyll *a*/*b* antenna complex. A serine-threonine protein kinase, STN7 in vascular plants (1) and Stt7 in green algae (2), is responsible for this phosphorylation. Stt7/STN7 activity depends on the redox state of the plastoquinone (PQ) pool, which is sensed by the cytochrome b_6f complex (3).

According to the current model of STs, preferential PSII excitation leads to PQ reduction, and thus to LHCII phosphorylation by the kinase. The PQ pool can also be reduced in dark anaerobic conditions in algal suspensions. In this state, called state 2 (S2), phosphorylated LHCII dissociates from PSII, thereby reducing its absorption cross-section, and associates to PSI, acting as an additional antenna for this complex. In the reverse process, preferential excitation of PSI oxidizes the PQ pool, inactivating Stt7/STN7 and leading to dephosphorylation of LHCII by a phosphatase. Dephosphorylated LHCII recouples to PSII [state 1 (S1)]. Although it is acknowledged that STs induce extensive supramolecular reorganizations of the PSs (reviewed in ref. 4), much less is known about possible changes in the thylakoid-membrane ultrastructure (5). In *Arabidopsis thaliana*, substantial changes in the stacking and major rearrangements of the entire thylakoid-membrane network were observed using electron microscopy (EM) on isolated thylakoid membranes (6). However, Fristedt et al. (7) found no connection between LHCII phosphorylation and changes in the thylakoid stacking and suggested that phosphorylation of the PSII core is responsible for the observed changes, again based on EM analysis. In the green alga *Chlamydomonas reinhardtii,* where ST is a prominent

Significance

Oxygenic photosynthesis regulates light–energy conversion by balancing the activity of the two photosystems (PSs). Such a power balance requires a sophisticated regulatory mechanism called state transitions, which involve reversible phosphorylation of the light-harvesting complex proteins (LHCIIs) to redistribute absorbed excitation energy between the two photosystems. Using noninvasive techniques (small-angle neutron scattering, circular dichroism, and absorption transient spectroscopy) in the green alga *Chlamydomonas reinhardtii*, we have revealed that state transitions modify the chloroplast structure, affecting the stacking and periodicity of the photosynthetic membranes and altering protein–protein interactions within these membranes. These structural changes accompany the conversion of LHCII into an energy-dissipating mode with only minor displacements of phosphorylated LHCIIs from PSII to PSI, thereby allowing us to reevaluate the physiological significance of state transitions.

Author contributions: G.N., G.G., G.F., and J.M. designed research; G.N., R.Ü., O.Z., R.T., K.T., L.P., L.M., D.P., G.G., G.F., and J.M. performed research; L.P. contributed new reagents/analytic tools; G.N., R.Ü., O.Z., R.T., D.P., G.G., G.F., and J.M. analyzed data; and G.N., G.G., G.F., and J.M. wrote the paper.

The authors declare no conflict of interest.

This article is a PNAS Direct Submission.

[1]To whom correspondence may be addressed. E-mail: minagawa@nibb.ac.jp, garab.gyozo@brc.mta.hu, or giovanni.finazzi@cea.fr.

This article contains supporting information online at www.pnas.org/lookup/suppl/doi:10.1073/pnas.1322494111/-/DCSupplemental.

process (8), EM data also suggest that thylakoid stacking is loosened in S2 (9). A major problem with these studies is that they are based on data collected on chemically fixed membranes. Therefore, (*i*) it is impossible to exclude artifacts during sample preparation, and (*ii*) no dynamic information is available. To overcome these difficulties, we developed an approach based on noninvasive techniques, such as small-angle neutron scattering (SANS), circular dichroism (CD), and time-resolved absorption spectroscopy, to investigate the consequences of STs on the chloroplast ultrastructure and function under physiologically relevant conditions, in living cells of the green alga *C. reinhardtii*.

SANS carries accurate structural information on the membrane ultrastructure (10). It requires neither staining, nor chemical, nor low-temperature fixation of the sample and therefore can be performed under physiologically relevant conditions in living cells, which can be illuminated during the measurements. In a series of SANS experiments on isolated thylakoids, cyanobacteria, and algae, repeat distances (RDs) of membranes were determined (11–13), and small (<20 Å) but well-discernible light-induced reversible RD changes were revealed on time scales of several minutes (11, 12). CD spectroscopy is another noninvasive technique, which provides information on the organization of the pigment systems in hierarchically organized molecular assemblies. Of particular interest, the giant, *psi*-type CD signal originates from ordered arrays of the individual pigment–protein complexes and is superimposed onto their individual CD signals (14). In multilamellar thylakoids, the *psi*-type CD is sensitive to both the lateral order of the complexes and the stacking of membranes and depends largely on the size of the macrodomains formed by the PSII–LHCII supercomplex (14, 15). Finally, the techniques of chlorophyll-*a* fluorescence and electrochromic absorption transients at room temperature have been extensively used in the past to characterize the functional and structural consequences of STs in vivo (8).

In this study, SANS and CD reveal regular thylakoid organization in S1, well-defined periodicity of the thylakoid membranes, and ordered arrays of PSII–LHCII supercomplexes, respectively. These features are largely diminished in S2, and the structural changes follow the same kinetics as STs. Direct assessment of the PSII and PSI antenna size in S1 and S2 confirms a large decrease of the PSII cross-section, which, however, does not bring about a commensurate increase of the PSI antenna. This conclusion is corroborated by direct measurements of antenna composition in the PSII–LHCII supercomplex. Therefore, by combining these approaches on living cells with biochemical analysis, we dissect both the structural and functional consequences of STs in *Chlamydomonas* in vivo.

Results

Small-Angle Neutron Scattering Measurements Indicate That State Transitions Modulate Thylakoid Stacking and Periodicity. Small-angle neutron scattering (SANS) is a noninvasive technique that offers the unique opportunity to study thylakoid ultrastructural changes in vivo (Fig. S1). We applied this technique to *Chlamydomonas* to investigate the structural consequences of this phenomenon in living cells. In this alga, electron microscopy shows stacks of 2–10 thylakoids (16), similar to those found in grana. Therefore, one can expect an RD of 160–180 Å and a Bragg peak between 0.035 and 0.039 $Å^{-1}$ (17), based on the Bragg equation RD = $2\pi/Q^*$, where Q^* is the position of a diffraction peak (Fig. 1*A*).

Well-defined Bragg diffraction peaks were previously reported between 0.02 and 0.035 $Å^{-1}$ in isolated granal chloroplasts, cyanobacteria, and diatoms (11, 18). However, SANS experiments on the dark-adapted WT *Chlamydomonas* cells could not reveal any distinct Bragg diffraction peak, but only a shoulder at ~0.035 $Å^{-1}$, indicating a poorly defined RD of ~180 Å (Fig. 1*B*, black curve). Conversely, the scattering profile was

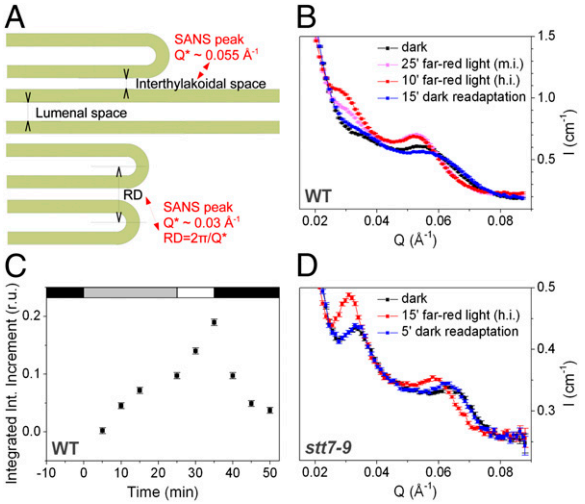

Fig. 1. Schematic drawing of thylakoid membranes (*A*) and SANS features in WT and *stt7-9* cells (*B–D*). (*A*) Simplified scheme showing the main structural parameters of the stacked thylakoid membranes and their relation to the Bragg diffraction peak at ~0.033 $Å^{-1}$, corresponding to an RD of ~190 Å, and to the peak at ~0.055 $Å^{-1}$, which is proposed to originate from the membrane pairs. (*B*) SANS profiles in the WT were recorded on cells adapted to dark (black), and during 25-min exposure to medium intensity (~0.3 $mW \cdot cm^{-2}$) (magenta) and high intensity (~1 $mW \cdot cm^{-2}$) (red) far-red light, inducing an S2-to-S1 transition. Reversibility was checked during 15-min dark readaptation (blue). Data-acquisition time for each measurement was 5 min. (*C*) Rise and decay of the Bragg peak at ~0.03 $Å^{-1}$, characterized by the increment of the integrated intensity of the SANS scattering curves in the 0.024–0.039 $Å^{-1}$ interval relative to the dark-adapted curve. The white, gray, and black bars at the top indicate far-red illumination at high intensity, medium intensity, and darkness, respectively. (*D*) SANS profiles of dark-adapted, far-red–illuminated, and dark-readapted *stt7-9* cells. Results are mean values ± SEM.

dominated by a peak at the higher momentum transfer (Q) region around 0.056 $Å^{-1}$ (Fig. 1*B*), which is tentatively assigned to originate from adjacent membrane pairs (ref. 11 and Fig. 1*A*). Due to the rather dense cell suspension (~10^8 cells·mL^{-1}), oxygen was consumed in the cuvette leading to anaerobic reduction of the PQ pool and consequent kinase activation. Thus, the dark-adapted cells were in S2 conditions proved by parallel measurements of the 77 K fluorescence spectra (Fig. S2*A*). Here, the amplitude of the PSI emission peak (λ ~712 nm) was much larger than that of PSII (λ ~685 and 695 nm). When the cell suspension was subjected to far-red light illumination within the neutron beam, a transition to S1 was observed (Fig. S2*A*). In this case, the appearance of a peak at around 0.029–0.032 $Å^{-1}$, corresponding to RD between 196 and 217 Å (Fig. 1*B*), indicates that recovery of S1 and recovery of thylakoid periodicity are linked. The amplitude of the Bragg peak depended on the intensity and duration of the illumination. The observed light effect was reversible, as the distinct Bragg peak disappeared when the cells were readapted to the dark anaerobic (S2) conditions. These findings were corroborated by parallel experiments where an S2-to-S1 transition was induced by exposing the cells to light in the presence of 3-(3,4-dichlorophenyl)-1,1-dimethylurea (DCMU), which inhibits electron transport between Q_A and Q_B and inactivates the STT7 kinase via the oxidation of the PQ pool in the light (19). Similar to using far-red illumination, we observed the emergence of the Bragg diffraction peak at around 0.03 $Å^{-1}$ (Fig. S3*A*, red curve). Again, the appearance of this peak was fully reversible in the dark. To further explore the relationship between STs and changes in thylakoid periodicity, we exploited the fact that SANS is a relatively fast technique compared with other structural approaches (one frame can be obtained in ~30 s on the

investigated system), and therefore it offers the unique opportunity to study the kinetics of thylakoid ultrastructural changes in vivo. Kinetics of structural changes are presented in Fig. 1*C*, which reveals that changes in the organization of the thylakoid membranes occur in the timescale of ∼10 min: i.e., in a time range comparable with that of the S2-to-S1 transition in *Chlamydomonas* (19).

Earlier experiments performed on cyanobacterial and diatom cells (11, 12, 18) have shown that light exposure induces dark-reversible changes in the thylakoid-membrane ultrastructure, affecting both the Bragg peaks and the high-Q peak, without inducing ST. To verify the existence of this phenomenon in *Chlamydomonas*, we performed experiments on the *stt7-9* mutant, which is unable to perform STs (20). In dark-adapted *stt7-9* cells, a strong Bragg peak at 0.033 $Å^{-1}$ (RD = 190 Å) was found (Fig. 1*D*), confirming that changes in the Bragg peak observed in the WT (either by far-red illumination or DCMU treatments) are intimately related to the occurrence of ST. On the other hand, illumination of *stt7* also produced a shift in the characteristic peaks toward lower Q values, to $Q^* = 0.031$ $Å^{-1}$ (RD = 203 Å), indicating that illumination per se induces an ∼10-Å increase in the RD in the thylakoid membranes. Also, the high-Q peak shifted to lower Q values from 0.065 to 0.058 $Å^{-1}$, indicating a small but well-discernible light-induced expansion of the characteristic distances, i.e., a swelling (11, 18). We noted that the Q values measured in *stt7-9* are higher than in the WT, which shifted from ∼0.056–0.053 $Å^{-1}$, consistent with a tighter organization and stronger stacking of the membranes in the mutant locked in S1. The same effects were observed in a double mutant *npq4 stt7-9* (Fig. S4), which, in addition to its incapability for ST, possesses a largely reduced qE capacity (20). Therefore, the light-induced increase of the RD of thylakoid membranes observed in the WT is not linked to qE, the energy-dependent nonphotochemical quenching mechanism. Variations in the SANS profiles in the diatom *Phaeodactilum tricornutum* are sensitive to changes in the osmolality of the medium (12). We observed the same phenomenon in *Chlamydomonas,* where both peaks gradually and reversibly shifted to higher Q values also upon gradually increasing the sorbitol concentration from 0 to 300 mM (Fig. S5), indicating shrinking of the thylakoids as expected and supporting our interpretation about the shift in the peak positions. Thus, we conclude that light promotes thylakoid swelling in *Chlamydomonas*.

CD Measurements Indicate Stronger Long-Range Order and Stacking in State 1. As a complementary approach to investigate the consequences of ST on the thylakoid structure in vivo, CD spectroscopy was used. In the red region of the visible spectrum of *C. reinhardtii* cells, intense *psi*-type CD bands at (−)675 and (+)690 nm, similar to vascular plants, were seen (Fig. 2). In plants, *psi*-type bands have been shown to be given rise by large (200–400 nm in diameter) ordered arrays of PSII–LHCII supercomplexes, the magnitude of which depends on their sizes (14). The self-assembly of these ordered macroarrays, enriched in PSII and LHCII and largely void of PSI complexes and the ATP synthase, constitutes the structural basis of the segregation of the two PSs, which, together with stacking, leads to the formation of the grana (21, 22).

For CD spectroscopy, cells were acclimated to S2 in the dark through N_2 bubbling because the concentration used for CD is much lower than for SANS, and therefore O_2 consumption through respiration is much slower. We observed a small but significant (∼20%) increase of the total amplitude of the red *psi*-type CD signals (i.e., the intensity difference of the positive and negative amplitudes) upon a transition from S2 to S1. On the other hand, this amplitude changed only marginally in *stt7-9* cells (Fig. 2*B*) as well as in *stt7-1* (Fig. S6), a clone that was initially isolated and characterized (2), confirming that changes were triggered by ST. The stronger *psi*-type signals in S1 than in S2 are consistent with earlier indications that the size of the macroarrays of PSII–LHCII

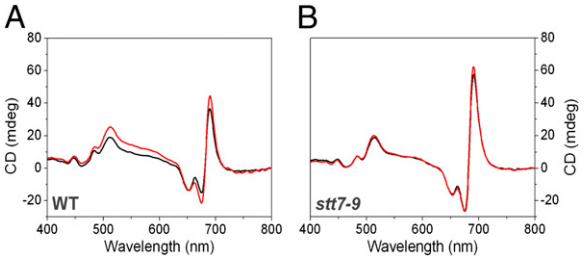

Fig. 2. CD spectra of WT (*A*) and *stt7-9* (*B*) cells in S1 (red) and S2 (black). Spectra were recorded at room temperature, baseline-corrected, and normalized to the same optical density of the samples (1.0 at the red maximum). The total amplitude of the *psi*-type signal (i.e., of the difference of the positive and negative amplitudes) following the preillumination of the cells with high-intensity (∼2.5 $mW \cdot cm^{-2}$) far-red light increased from 55.3 ± 8.0 (dark anaerobic, S2) to 66.1 ± 6.2 mdeg (far-red preilluminated aerobic, S1) in the WT and from 99.7 ± 6.8 mdeg to 105.1 ± 6.3 mdeg in the S1-locked *stt7-9* cells, which received the same treatments at 25 °C for 30 min (mean values ± SEM from four independent experiments, on different batches).

supercomplexes is larger in stacked than in unstacked membranes (14). Consistent with this observation, the amplitude of the (−)675-nm *psi*-type band, relative to the (−)650-nm excitonic band, is more pronounced in S1 than in S2 (Fig. 2*A*). The (−)675-nm *psi*-type band has earlier been shown to be associated with the stacking of membranes (15). Therefore, these data show that, in accordance with earlier EM data and our SANS experiments, the S1-to-S2 transition partially unstacks the thylakoids and modifies the arrangement of the photosynthetic complexes in the membrane. However, the finding that ST from S1 to S2 only diminishes, but does not eliminate, the *psi*-type signals that originate from ordered PSII–LHCII macroarrays is intriguing because it indicates that a significant part of the PSII–LHCII supercomplexes is maintained in S2. If a huge membrane reorganization had occurred during an S1-to-S2 transition, with ∼80% of LHCII migrating from PSII to PSI (23), much larger changes should have been observed in the CD.

Consequences of STs on the PSII and PSI Antenna. The above mentioned CD results prompted us to reexamine the relationship between ST and the changes in the PSI and PSII antenna sizes using (again) a noninvasive approach in vivo based on fluorescence and visible absorption spectroscopy. We first assessed changes in the PSII antenna size by quantifying the variation in the maximum Fm level in S2 and S1 conditions in the presence of DCMU. Because PSII photochemistry is blocked at Fm by the inhibitor, changes in fluorescence reflect changes in its light-harvesting capacity. We confirmed that a transition from S2 to S1, here achieved by illumination of dark-adapted anaerobic cells poised with DCMU, was accompanied by a large (almost twofold) increase of the Fm yield at room temperature (Fig. 3*A*). A calculation made using the changes of the variable fluorescence (i.e., the fraction of fluorescence that arises only from PSII) in S1 and S2 indicates that ∼75% of the PSII antenna is "quenched" in the latter state. In principle, this calculation is consistent with previous conclusions that a large fraction of the PSII antenna (functionally) detaches from this complex during ST in *Chlamydomonas* (23). In parallel, we measured changes in the PSI antenna size using the electrochromic shift (ECS) of photosynthetic pigments as a probe (24). This signal reflects a shift in the absorption spectrum of membrane-embedded pigments, caused by the generation of a transmembrane electrical field in the light (24). We found that the initial slope of the ECS changes measured in continuous light and in the presence of DCMU to inhibit PSII was proportional to the light intensity (Fig. S7): i.e., it can be used to probe the absorption cross-section

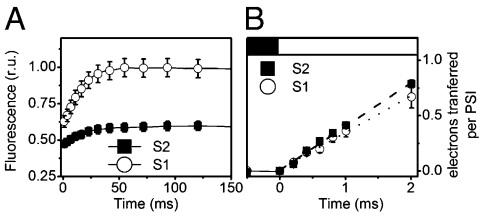

Fig. 3. Determination of PSII and PSI antenna sizes in S2 and S1. S2 was obtained through anaerobic incubation in the dark for 30 s whereas S1 was induced by illumination of DCMU-poisoned cells. (*A*) Maximum fluorescence yield (Fm) under both S2 and S1 promoting conditions in DCMU-poisoned cells, a method to estimate the PSII antenna size. (*B*) ECS absorbance transients in DCMU (40 μM)-hydroxylamine (1 mM)-poisoned cells in S2 and S1 conditions. The initial rate of this signal is proportional to the antenna size of PSI (Fig. S7). Data refer to mean values ± SEM from three independent experiments on different batches. The concentration was 2×10^7 cells·mL^{-1}.

of PSI (25). When tested under the same conditions used to modify the PSII antenna size, only very minor changes in the initial slope of the ECS were found (~15%) (Fig. 3*B*), in agreement with recent reports by Takahashi et al. (25) (~25%). This conclusion was further supported by similar measurements performed in the *ac208* mutant, which cannot perform electron flow because it lacks plastocyanin (26) but undergoes a large state transition depending on redox conditions. In this strain, too, a large quenching was observed in PSII (Fig. S8*C*) with small effects (less than 20%) on the PSI absorption cross-section (Fig. S9*C*). On the other hand, no such changes were seen in the *stt7* strains (Figs. S8 *A* and *B* and S9 *A* and *B*), indicating that they reflect a genuine change in the PSI antenna size due to LHCII association to this complex. Thus, we confirm by means of ECS kinetics measurements that the relatively small increase of the PSI absorption capacity upon a transition to S2 is not commensurate with large changes in the PSII absorption capacity.

Given the above, we reinvestigated the conventional view that all of the phosphorylated LHCIIs get dissociated from PSII and reassociate with PSI during ST in *Chlamydomonas*, which was done by characterizing PSII–LHCII supercomplex, using a purification method reported previously (27). There, the typical five green bands, including free LHCII (monomer and trimer), PSI–LHCI supercomplex, PSII–LHCII supercomplex, and PSI–LHCI–LHCII supercomplex (CEF supercomplex) (28), were obtained from the solubilized thylakoid membranes from the S2-locked cells (Fig. 4*A*, *Right*). LHCII proteins, as represented by one of the most abundant LHCII proteins LhcbM6, were distributed over free LHCII (51%), PSII–LHCII supercomplex (40%), and PSI–LHCI–LHCII supercomplex (9%) under S2 conditions (Fig. 4*B*, *Left*). Thus, it appears that a large fraction of LHCII proteins did not migrate to PSI but remained associated with PSII–LHCII supercomplex or in a free form after phosphorylation under S2 conditions, in agreement with the CD results indicating that the long-range order arrangement of the photosynthetic complexes was largely preserved in S2. Immunoblotting analysis of these fractions using anti-phosphothreonine antibody (Fig. 4*B*, *Right*) revealed that most of the phosphorylated LHCIIs are either in the fractions of free LHCII (54%) or PSII–LHCII supercomplex (44%) and that only 2% was associated with PSI–LHCI–LHCII supercomplex, suggesting that a large fraction of LHCII within the PSI–LHCI–LHCII supercomplex was not phosphorylated. It remains to be clarified that these LHCIIs never became phosphorylated or were dephosphorylated owing to their reassociation with PSI.

Discussion

In this work, we investigated the consequences of STs on the chloroplast thylakoid membranes in living cells. *C. reinhardtii* was chosen as a model because this alga has a very large ST capacity (23) and has been extensively used in the past to study this mechanism and its consequences (8). By combining structural and functional noninvasive approaches, we found that STs deeply affect the organization of chloroplast thylakoid membranes by introducing reorganizations at different levels of the structural complexity.

The Thylakoid Ultrastructure Changes Following STs in Vivo. First, we provide clear in vivo evidence that ST leads to deep changes in the chloroplast thylakoid membranes. Our SANS data indicate a lower degree of stacking in S2 than in S1, consistent with earlier EM data in isolated plant thylakoids (6) and algae (29). However, using a noninvasive approach in living cells, we were able to exclude the possibility that the observed structural changes were artifacts: e.g., due to sample preparation for EM analysis. More importantly, the SANS data show that a transition from S1 to S2 essentially eliminates the periodic arrangement of

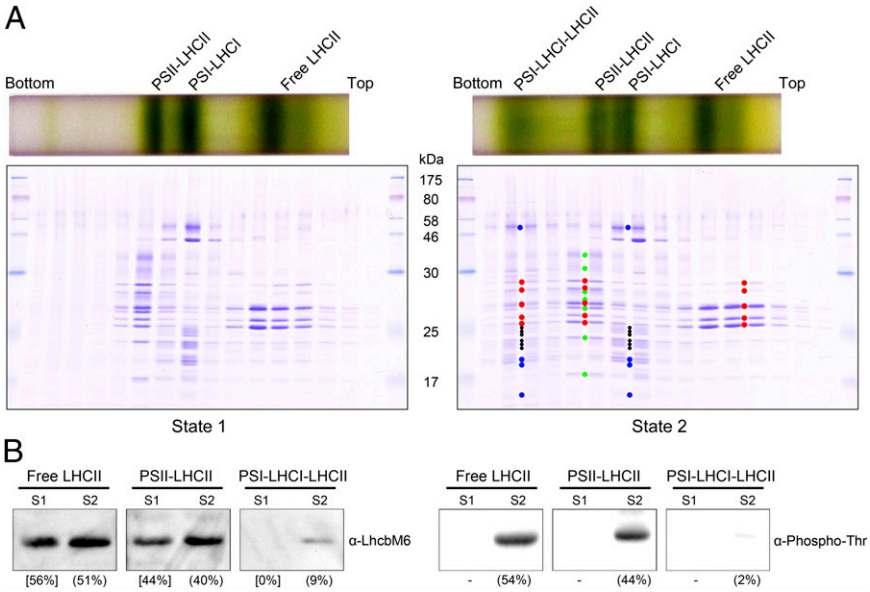

Fig. 4. Distributions of LHCII proteins among the photosynthetic complexes during STs. (*A*) Sucrose density gradient centrifugation (*Upper*) followed by SDS/PAGE analysis (*Lower*). Protein bands were stained with Coomassie Brilliant Blue R-250. Red dots (from top), CP26, CP29, LHCII type I (LhcbM3/4/6/8/9), type IV (LhcbM1), and type III (LhcbM2/7); blue dots (from top), PsaA/B, PsaD, PsaF, and PsaE; black dots (from top), Lhca4, -6, -3, -2, -5, and -7/8; green dots (from top), CP47, CP43, D2, D1, PsbO, PsbP, and PsbQ. (*B*) Immunoblot analysis of a major LHCII protein LhcbM6 (*Left*) and phosphorylated LHCII proteins (*Right*) within the photosynthetic complexes from S1 and S2 *C. reinhardtii* cells. Numbers with brackets and parentheses show relative band intensities among S1 and S2 samples, respectively.

the thylakoid membranes (Fig. 1), thereby revealing a more extensive membrane reorganization than unstacking. Indeed, unstacking, per se, would just increase the RD and would not explain the absence of a distinct Bragg diffraction peak (11, 18). Further, because SANS is a relatively fast technique, we were able to show that structural changes follow similar kinetics as the changes in the room-temperature fluorescence of PSII, which are commonly used to assess the dynamics of ST in vivo (4, 30). Therefore, we conclude that overall ultrastructural changes and ST are intimately linked and most likely mechanistically related.

Furthermore, our in vivo analysis also reveals other light-induced structural changes unrelated to ST. Illumination causes a partial expansion of the RDs, which might originate from the expansion of either the interthylakoidal space or the lumen, or from the expansion of both (11, 12, 18, 31). Because these changes are also seen in mutants devoid of ST (*stt7-9* mutant in Fig. 1) and devoid of both ST and qE (*npq4 stt7-9* double mutant in Fig. S4), we conclude that these membrane reorganizations are not triggered by STs or qE. However, by enhancing the mobility of membrane proteins, these changes might be involved in the regulation of the thylakoid ultrastructure and thus could also provide the molecular bases for migration of a fraction of the phosphorylated LHCIIs out of the stacked membranes during ST.

Consequences of STs on PSII and PSI Antenna Size. Our noninvasive study provides invaluable insights into the functional consequences of STs on the antenna of the two PSs, including structural information gained in vivo. As indicated by the presence of a large *psi*-type CD signal in both S1 and S2 (Fig. 2), the number or size of arrays of the PSII–LHCII supercomplexes in the membranes was diminished, but each unit of the PSII–LHCII supercomplexes was not dismantled during a transition from S1 to S2. These data imply that the PSII–LHCII macrodomains are largely preserved in S2, contrasting with the notion that almost all of the LHCIIs leave this complex and reassociate with PSI during ST in *Chlamydomonas*. Much larger diminishments of the *psi*-type CD signals were found in the *koLhcb6* and *koPsbW* mutants, where the organization and stability of PSII–LHCII supercomplexes are perturbed (32, 33). Overall, the small decrease in the characteristic intensities of the *psi*-type CD signal (~20%) suggests that only a limited amount of LHCII physically dissociated from PSII in S2, in agreement with our estimates of the relative increase of the PSI antenna using time-resolved ECS spectroscopy (~15%) (Fig. 3*B*) and our biochemical analysis of the PSII–LHCII supercomplex in S2 (Fig. 4). On the other hand, we suggested that a large fraction of the PSII–LHCII supercomplexes and or LHCIIs become quenched in S2, as shown by the ~75% quenching of variable PSII fluorescence at room temperature in S2. To rationalize these apparently contrasting results, we propose a model where a large part of the LHCIIs become phosphorylated in S2, and only a part of them, possibly those located at the periphery of the supercomplex, migrate to PSI (Fig. 4). The remaining ones either bound to PSII or unbound are left in an energetically quenched state (Fig. 3*A*). We see functional similarities between these quenched LHCIIs and the ones previously observed upon the formation of qE (34), and the quenched LHCII complexes detected by FLIM (fluorescence lifetime image microscopy) analysis of *Chlamydomonas* cells during ST (29). It is of note that the recently discovered key protein for qE, LHCSR3 (27, 35), was not expressed under the conditions tested in this study, where the cells were grown in the presence of acetate under low light. Thus, the quenching effect observed here cannot be mediated by LHCSR3. The above scenario for ST (Fig. 5) allows unifying different views concerning this process proposed previously. We reach similar conclusions as Delosme et al. (23) concerning PSII, while integrating the idea of Iwai et al. (29) that ST leads to the formation of quenched LHCII in vivo. Moreover, our data support recent findings that S- and M-trimers of LHCII stay on PSII upon phosphorylation in plants (36), while confirming that some LHCII becomes an efficient PSI antenna in S2, as proposed in ref. 37.

Physiology of ST Revisited. Overall, our data have allowed us to propose a general model for STs, which is applicable to both plants and algae; the model accounts for not only the major features of ST in the light, but also those in the dark (aerobic vs. anaerobic conditions). We conclude that the consequences of ST on the antenna size of PSI are small (around 20%) in both light (8) and anaerobic (this study) conditions. In the light, the functional size of the PSII antenna is decreased by a similar extent in plants and green algae (8, 38) and its changes are similar to the increase in the PSI antenna. Thus, STs serve the purpose of balancing light utilization by the two PSs for optimal photosynthesis under these conditions. However, a much larger decrease of the PSII antenna is specifically seen in *Chlamydomonas* under anaerobic conditions (50%), likely representing a specific means of down-regulating PSII under conditions where its activity must be lowered to avoid interference

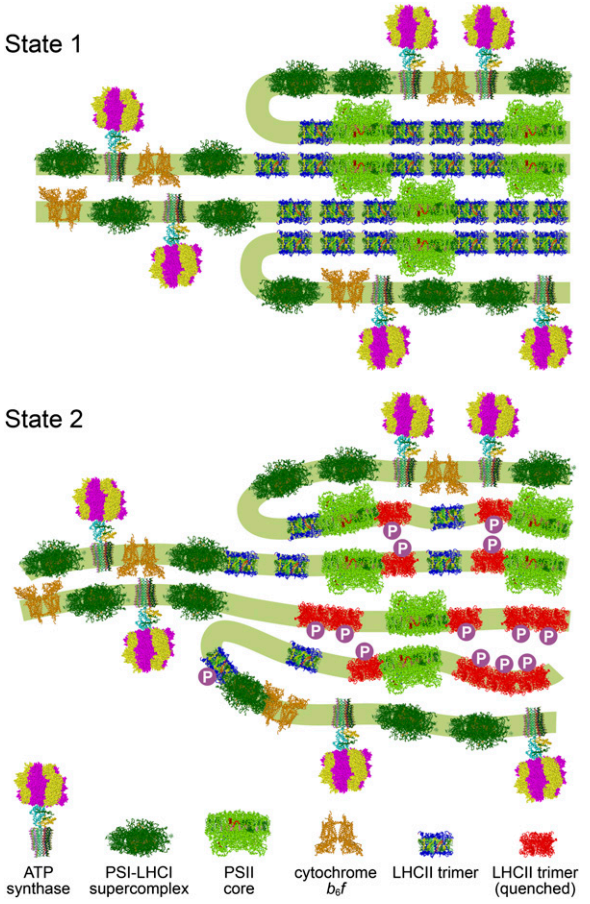

Fig. 5. Hypothetical model for the chloroplast remodeling during STs in *C. reinhardtii*. Side views of the membrane planes showing alterations in the thylakoid ultrastructure and photosystem supercomplex composition. For S1 (*Upper*), thylakoids are more stacked, and large arrays of PSII–LHCII supercomplexes reside in the appressed regions. The periodicity (RD) of thylakoid membranes is well-defined. PSI–LHCI supercomplexes, cytochrome b_6f complexes, and ATP synthases are in the nonappressed regions. For S2 (*Lower*), a number of LHCII proteins are phosphorylated, and the thylakoids are partially unstacked and undulated. The periodicity of the thylakoid membranes is weak. Most of the phosphorylated LHCIIs are in energy-quenching state (red). They either remain associated with PSII so that a large part of the PSII–LHCII supercomplex array is preserved, or are unbound and aggregated. Unphosphorylated LHCIIs and LHCIIs bound to PSI are still actively harvesting light (blue).

with the specific physiological responses to anaerobiosis (induction of cyclic electron flow around PSI, H_2 production) of this alga (8), which are all inhibited by PSII activity. Reversible inactivation of most of the PSII antenna would represent a fast and energetically cheap way to minimize PSII activity without excessively increasing PSI excitation. A recent report has indeed shown that when PSI cannot evacuate electrons, due to its excitation being higher than the capacity to use electrons at its acceptor side (e.g., in anaerobiosis) (25), the complex becomes locked in a closed state where recombination is enhanced and possible photodamage ensues. We conclude that STs in *C. reinhardtii* modify the chloroplast structure, affecting the stacking and periodicity of the photosynthetic membranes, whereby LHCII is converted into an energy dissipating mode with only a minor movement of its phosphorylated form from PSII and PSI.

Materials and Methods

C. reinhardtii cells were routinely cultivated at 50 μmol photons·m^{-2}·s^{-1} in mixotrophic (Tris Acetate Phosphate medium) (39) conditions under continuous shaking. CD spectra were recorded between 800 and 400 nm using a Jasco J-815 CD spectrometer at room temperature (25 °C) with a bandwidth of 5 nm and a scanning speed of 100 nm/min (12). The 77 K fluorescence spectra were measured with a CCD array as previously described (20). Small-angle neutron scattering experiments were performed on the D22 SANS instrument at the Institut Laue-Langevin as described earlier (11) and in *SI Materials and Methods*. Absorption spectroscopy was performed with a JTS-10 spectrophotometer (Biologic France) as described in *SI Materials and Methods*. Thylakoid membranes were prepared from *C. reinhardtii* cells in S1 or S2 according to ref. 28. Photosynthetic supercomplexes were fractionated by sucrose density gradient after solubilizing the thylakoid membranes with *n*-dodecyl-α-D-maltoside as described previously (40). SDS/PAGE and immunoblottings with anti-LhcbM6 and phosphothreonine antibodies were performed as described (41).

ACKNOWLEDGMENTS. We thank the Institut Laue-Langevin and the Budapest Neutron Centre for providing beam time. We thank Drs. Michael Haertlein, Martine Moulin, Trevor Forsyth, and Philip Callow (Institut Laue-Langevin) for experimental help and György Káli (Wigner Research Centre for Physics) for suggestions about data interpretation. We also thank Sandrine Bujaldon (Institut de Biologie Physico Chimique) for providing the ac208 strain. We acknowledge Grants EU FP MC ITN "HARVEST" (to G.G.) and OTKA/NKTH-NIH (60003-00) (to G.G. and Dr. László Rosta), and NKTH-NIH (NAP-VENEUS05) (to Dr. László Rosta). G.F. and D.P. thank the Marie Curie Initial Training Network Accliphot (FP7-PEPOPLE-2012-ITN; 316427), the French National Agency "DiatomOil" Project (ANR-12-BIME-0005), and the Labex GRAL (Grenoble Alliance for Integrated Structural Cell Biology; ANR-10-LABEX-04). R.T. thanks the Japan Society for Grants-in-Aid for Research Activity Start-up (23870033). J.M. thanks the Cabinet Office for the Funding Program for Next Generation World-Leading Researchers (GS026), the Ministry of Education, Culture, Sports, Science and Technology for NC-CARP, and the New Energy and Industrial Technology Development Organization for the strategic development of next-generation bioenergy utilization technology (P07015).

1. Bellafiore S, Barneche F, Peltier G, Rochaix JD (2005) State transitions and light adaptation require chloroplast thylakoid protein kinase STN7. *Nature* 433(7028):892–895.
2. Depège N, Bellafiore S, Rochaix JD (2003) Role of chloroplast protein kinase Stt7 in LHCII phosphorylation and state transition in *Chlamydomonas*. *Science* 299(5612):1572–1575.
3. Wollman FA, Lemaire C (1988) Studies on kinase-controlled state transitions in photosystem-II and b6f mutants from *Chlamydomonas reinhardtii* which lack quinone-binding proteins. *Biochim Biophys Acta* 933(1):85–94.
4. Minagawa J (2011) State transitions: The molecular remodeling of photosynthetic supercomplexes that controls energy flow in the chloroplast. *Biochim Biophys Acta* 1807(8):897–905.
5. Tikkanen M, Suorsa M, Gollan PJ, Aro EM (2012) Post-genomic insight into thylakoid membrane lateral heterogeneity and redox balance. *FEBS Lett* 586(18):2911–2916.
6. Chuartzman SG, et al. (2008) Thylakoid membrane remodeling during state transitions in *Arabidopsis*. *Plant Cell* 20(4):1029–1039.
7. Fristedt R, et al. (2009) Phosphorylation of photosystem II controls functional macroscopic folding of photosynthetic membranes in *Arabidopsis*. *Plant Cell* 21(12):3950–3964.
8. Eberhard S, Finazzi G, Wollman FA (2008) The dynamics of photosynthesis. *Annu Rev Genet* 42(1):463–515.
9. Iwai M, Takahashi Y, Minagawa J (2008) Molecular remodeling of photosystem II during state transitions in *Chlamydomonas reinhardtii*. *Plant Cell* 20(8):2177–2189.
10. Fitter J, Gutberlet T, Katsaras J (2006) *Neutron Scattering in Biology* (Springer, Berlin).
11. Nagy G, et al. (2011) Reversible membrane reorganizations during photosynthesis in vivo: revealed by small-angle neutron scattering. *Biochem J* 436(2):225–230.
12. Nagy G, et al. (2012) Modulation of the multilamellar membrane organization and of the chiral macrodomains in the diatom *Phaeodactylum tricornutum* revealed by small-angle neutron scattering and circular dichroism spectroscopy. *Photosynth Res* 111(1-2):71–79.
13. Posselt D, et al. (2012) Small-angle neutron scattering study of the ultrastructure of chloroplast thylakoid membranes: Periodicity and structural flexibility of the stroma lamellae. *Biochim Biophys Acta* 1817(8):1220–1228.
14. Garab G, van Amerongen H (2009) Linear dichroism and circular dichroism in photosynthesis research. *Photosynth Res* 101(2-3):135–146.
15. Garab G, Kieleczawa J, Sutherland JC, Bustamante C, Hind G (1991) Organization of pigment protein complexes into macrodomains in the thylakoid membranes of wild-type and chlorophyll-*b*-less mutant of barley as revealed by circular-dichroism. *Photochem Photobiol* 54(2):273–281.
16. Goodenough UW, Staehelin LA (1971) Structural differentiation of stacked and unstacked chloroplast membranes: Freeze-etch electron microscopy of wild-type and mutant strains of *Chlamydomonas*. *J Cell Biol* 48(3):594–619.
17. Diederichs K, Welte W, Kreutz W (1985) Determination of interaction forces between higher-plant thylakoids and electron-density-profile evaluation using small-angle x-ray-scattering. *Biochim Biophys Acta* 809(1):107–116.
18. Liberton M, et al. (2013) Organization and flexibility of cyanobacterial thylakoid membranes examined by neutron scattering. *J Biol Chem* 288(5):3632–3640.
19. Delepelaire P, Wollman FA (1985) Correlations between fluorescence and phosphorylation changes in thylakoid membranes of *Chlamydomonas reinhardtii* in vivo: A kinetic analysis. *Biochim Biophys Acta* 809(2):277–283.
20. Allorent G, et al. (2013) A dual strategy to cope with high light in *Chlamydomonas reinhardtii*. *Plant Cell* 25(2):545–557.
21. Dekker JP, Boekema EJ (2005) Supramolecular organization of thylakoid membrane proteins in green plants. *Biochim Biophys Acta* 1706(1-2):12–39.
22. Mustárdy L, Buttle K, Steinbach G, Garab G (2008) The three-dimensional network of the thylakoid membranes in plants: Quasihelical model of the granum-stroma assembly. *Plant Cell* 20(10):2552–2557.
23. Delosme R, Olive J, Wollman FA (1996) Changes in light energy distribution upon state transitions: An in vivo photoacoustic study of the wild type and photosynthesis mutants from *Chlamydomonas reinhardtii*. *Biochim Biophys Acta* 1273(2):150–158.
24. Bailleul B, Cardol P, Breyton C, Finazzi G (2010) Electrochromism: A useful probe to study algal photosynthesis. *Photosynth Res* 106(1-2):179–189.
25. Takahashi H, Clowez S, Wollman FA, Vallon O, Rappaport F (2013) Cyclic electron flow is redox-controlled but independent of state transition. *Nat Commun* 4:1954.
26. Quinn J, et al. (1993) The plastocyanin-deficient phenotype of *Chlamydomonas reinhardtii* Ac-208 results from a frame-shift mutation in the nuclear gene encoding preapoplastocyanin. *J Biol Chem* 268(11):7832–7841.
27. Tokutsu R, Minagawa J (2013) Energy-dissipative supercomplex of photosystem II associated with LHCSR3 in *Chlamydomonas reinhardtii*. *Proc Natl Acad Sci USA* 110(24):10016–10021.
28. Iwai M, et al. (2010) Isolation of the elusive supercomplex that drives cyclic electron flow in photosynthesis. *Nature* 464(7292):1210–1213.
29. Iwai M, Yokono M, Inada N, Minagawa J (2010) Live-cell imaging of photosystem II antenna dissociation during state transitions. *Proc Natl Acad Sci USA* 107(5):2337–2342.
30. Rochaix JD, et al. (2012) Protein kinases and phosphatases involved in the acclimation of the photosynthetic apparatus to a changing light environment. *Philos Trans R Soc Lond B Biol Sci* 367(1608):3466–3474.
31. Kirchhoff H, et al. (2011) Dynamic control of protein diffusion within the granal thylakoid lumen. *Proc Natl Acad Sci USA* 108(50):20248–20253.
32. Kovács L, et al. (2006) Lack of the light-harvesting complex CP24 affects the structure and function of the grana membranes of higher plant chloroplasts. *Plant Cell* 18(11):3106–3120.
33. García-Cerdán JG, et al. (2011) The PsbW protein stabilizes the supramolecular organization of photosystem II in higher plants. *Plant J* 65(3):368–381.
34. Jahns P, Holzwarth AR (2012) The role of the xanthophyll cycle and of lutein in photoprotection of photosystem II. *Biochim Biophys Acta* 1817(1):182–193.
35. Peers G, et al. (2009) An ancient light-harvesting protein is critical for the regulation of algal photosynthesis. *Nature* 462(7272):518–521.
36. Wientjes E, Drop B, Kouřil R, Boekema EJ, Croce R (2013) During state 1 to state 2 transition in *Arabidopsis thaliana*, the photosystem II supercomplex gets phosphorylated but does not disassemble. *J Biol Chem* 288(46):32821–32826.
37. Galka P, et al. (2012) Functional analyses of the plant photosystem I-light-harvesting complex II supercomplex reveal that light-harvesting complex II loosely bound to photosystem II is a very efficient antenna for photosystem I in state II. *Plant Cell* 24(7):2963–2978.
38. Ebenhoh OFJ, Finazzi G, Rochaix JD, Goldschmidt-Clermont M (2013) Short-term acclimation of the photosynthetic electron transfer chain to changing light: A mathematical model. *Phil Trans R Soc B* 369(1640):20130223.
39. Gorman DS, Levine RP (1965) Cytochrome f and plastocyanin: Their sequence in the photosynthetic electron transport chain of Chlamydomonas reinhardi. *Proc Natl Acad Sci USA* 54(6):1665–1669.
40. Tokutsu R, Kato N, Bui KH, Ishikawa T, Minagawa J (2012) Revisiting the supramolecular organization of photosystem II in *Chlamydomonas reinhardtii*. *J Biol Chem* 287(37):31574–31581.
41. Tokutsu R, Iwai M, Minagawa J (2009) CP29, a monomeric light-harvesting complex II protein, is essential for state transitions in *Chlamydomonas reinhardtii*. *J Biol Chem* 284(12):7777–7782.